FEATURE ARTICLE

Uncovering the Fundamental Chemistry of Alkyl + O_2 Reactions via Measurements of Product Formation

Craig A. Taatjes

Combustion Research Facility, Mail Stop 9055, Sandia National Laboratories, Livermore, California 94551-0969

Received: December 1, 2005

The reactions of alkyl radicals (R) with molecular oxygen (O_2) are critical components in chemical models of tropospheric chemistry, hydrocarbon flames, and autoignition phenomena. The fundamental kinetics of the R + O_2 reactions is governed by a rich interplay of elementary physical chemistry processes. At low temperatures and moderate pressures, the reactions form stabilized alkylperoxy radicals (RO_2), which are key chain carriers in the atmospheric oxidation of hydrocarbons. At higher temperatures, thermal dissociation of the alkylperoxy radicals becomes more rapid and the formation of hydroperoxyl radicals (HO_2) and the conjugate alkenes begins to dominate the reaction. Internal isomerization of the RO_2 radicals to produce hydroperoxyalkyl radicals, often denoted by QOOH, leads to the production of OH and cyclic ether products. More crucially for combustion chemistry, reactions of the ephemeral QOOH species are also thought to be the key to chain branching in autoignition chemistry. Over the past decade, the understanding of these important reactions has changed greatly. A recognition, arising from classical kinetics experiments but firmly established by recent high-level theoretical studies, that HO_2 elimination occurs directly from an alkylperoxy radical without intervening isomerization has helped resolve tenacious controversies regarding HO_2 formation in these reactions. Second, the importance of including formally direct chemical activation pathways, especially for the formation of products but also for the formation of the QOOH species, in kinetic modeling of R + O_2 chemistry has been demonstrated. In addition, it appears that the crucial rate coefficient for the isomerization of RO_2 radicals to QOOH may be significantly larger than previously thought. These reinterpretations of this class of reactions have been supported by comparison of detailed theoretical calculations to new experimental results that monitor the formation of products of hydrocarbon radical oxidation following a pulsed-photolytic initiation. In this article, these recent experiments are discussed and their contributions to improving general models of alkyl + O_2 reactions are highlighted. Finally, several prospects are discussed for extending the experimental investigations to the pivotal questions of QOOH radical chemistry.

Introduction

For decades, the reactions of alkyl radicals with molecular oxygen have been a subject of great interest and controversy. Interest in these reactions is motivated by their key role in atmospheric chemistry, low-temperature hydrocarbon oxidation, and autoignition processes; that interest is sustained by the intricacies of their fundamental chemistry. The general mechanism of an alkyl + O_2 reaction can be schematically represented as

$$\begin{array}{ccccccc} & & HO_2 + \text{alkene} & & & & \\ & & \uparrow & & \uparrow & & \\ R + O_2 & \longleftrightarrow & RO_2^{\#} & \longleftrightarrow & QOOH^{\#} & \longrightarrow & OH + \text{cyclic ether} \\ & & \updownarrow & & \updownarrow & & \\ & & RO_2 & & QOOH & & \end{array} \quad (1)$$

where # designates a chemically activated species. The reaction of an alkyl radical (R) with O_2 forms alkylperoxy radicals (RO_2) at low temperatures and moderate pressures. Alkylperoxy radicals are important intermediates in the oxidation of hydrocarbons in the troposphere.[1] However, it is the role of the alkyl + O_2 reaction in combustion chemistry that has focused attention on the complicated mechanism of these reactions.[2,3]

At higher temperatures (or very low pressures), the formation of bimolecular products such as HO_2 + alkenes or OH + cyclic ethers begins to dominate the reaction. The RO_2 radical can undergo internal H-abstraction to produce a hydroperoxyalkyl radical (QOOH), which can then dissociate to form OH or HO_2. These isomerizations occur via ring-shaped transition states; the isomerization through a six-membered ring is thought to be particularly facile.[3,4] The temperature regime where the major channel of the reaction changes from RO_2 to bimolecular products is sometimes called the transition region; this is where the consumption of alkyl radicals and the formation of products is not describable by a simple single rate coefficient but is a complicated convolution of stabilization, dissociation, and elimination processes.[5,6] In this region, typically from about 600 K to about 800 K, the microscopic behavior of the alkyl + O_2 reactions, especially the distribution among the various product channels, has a marked effect on chain branching and hence on

10.1021/jp056997f CCC: $33.50
Published on Web 03/01/2006

Craig Taatjes received a B.S. in chemistry in 1985 from Calvin College and a Ph.D. in chemical physics in 1991 from the University of Colorado, working under the supervision of Prof. Stephen R. Leone. He worked as a postdoctoral associate in Amsterdam at the Vrije Universiteit, with Prof. Steven Stolte, and at the FOM Institute for Atomic and Molecular Physics (AMOLF), with Prof. Aart W. Kleyn. In 1994, he joined the Combustion Research Facility of Sandia National Laboratories, in Livermore, California, where he is now a principal member of the technical staff. His research interests include fundamental flame chemistry and the kinetics of elementary reactions that are important in combustion.

ignition processes.[7,8] At these temperatures, the production of HO_2 and an alkene is essentially a chain-termination step, as the HO_2 radical is relatively inert. The production of a reactive OH radical facilitates chain propagation. The formation of the QOOH species is the key to chain branching at low temperature. Because the hydroperoxyalkyl species is a carbon-centered radical, it can add a second O_2 molecule, eventually producing two OH molecules and an alkoxy (RO) radical. Understanding the isomerization step to QOOH is therefore one of the major goals of R + O_2 investigations. However, the QOOH species is unstable and has never been directly observed; inferences as to its formation and reactivity remain indirect.

The mechanism for HO_2 formation in the R + O_2 reaction has historically been the source of some controversy. Early researchers considered that HO_2 + alkene could be a product of a direct abstraction reaction between O_2 and the alkyl radical,[9,10] which should have a substantial activation energy. In this case, the formation of alkylperoxy radicals and alkenes would proceed in parallel during the oxidation of alkyl radicals. Measurements that appeared to show ethene yields in the reaction of ethyl with O_2 decreasing to a plateau at ~0.06 as the pressure was increased[11] seemed to support this "parallel" mechanism. However, subsequent yield measurements over a wider range of pressures by Kaiser and co-workers[12−14] observed no plateau and demonstrated that the production of ethene in this reaction is dominated by a "coupled" mechanism in which bimolecular products arise through the formation of an alkylperoxy radical intermediate. In addition, measurements of the temperature dependence of R + O_2 reactions[3,4,15−20] have established that reactions to form HO_2 + alkene have negative activation energies, inconsistent with production via a direct abstraction mechanism.

The acceptance of the coupled mechanism did not solve the controversy over the mechanism of HO_2 formation, however. It was widely thought[9,19,20] that the isomerization to a QOOH species was preliminary to HO_2 formation. This presumption, combined with the observed negative activation energy for HO_2 + alkene production, would necessitate that energetic barriers to the RO_2 ↔ QOOH isomerization and to the dissociation of QOOH to HO_2 + alkene lie near or below the energy of the R + O_2 reactants. However, extensive work by Walker and co-workers[3,4,21−25] on the reverse reactions, the addition of HO_2 to alkenes, suggested a significant activation energy, large enough that the barrier to addition (and hence the transition state for dissociation of QOOH to HO_2 + alkene) must lie well above the R + O_2 asymptote. Walker and co-workers[4,18,25] proposed that the formation of HO_2 and the conjugate alkene must proceed directly from the RO_2 radical without isomerization to a QOOH species. This view has been vindicated by subsequent experiment[14,26−30] and high-level quantum chemical calculations.[5,6,31,32]

The establishment of the feasibility of direct elimination of HO_2 from alkylperoxy radicals arose from a focus on the C_2H_5 + O_2 reaction;[31,32] the theoretical unfolding of this model is discussed in a feature article in the *Journal of Physical Chemistry A* from the year 2000.[32] The C_2H_5 + O_2 reaction has been the subject of the most study of any R + O_2 reaction, and the understanding of its mechanism is the most mature. It is the smallest alkyl radical oxidation reaction for which the key pathways of HO_2 elimination and QOOH formation are possible, and because of its relative theoretical tractability, there has been a strong desire to treat it as a prototype for R + O_2 systems. However, the most important isomerization pathways to QOOH are likely those that proceed via six-membered ring transition states—a pathway that does not exist in the ethylperoxy radical—and the propyl radical reactions with oxygen are much better prototypes for general R + O_2 reactions.

The internal isomerization of alkylperoxy radicals to hydroperoxyalkyl radicals, and their subsequent dissociation to form OH and cyclic ethers, was deduced on the basis of measurements of cyclic ether production in hydrocarbon oxidation.[33,34] The work of Walker's group[3] has yielded a systematic description of the relative yields of cyclic ether and alkene products from alkyl + O_2 reactions. Under conditions where the removal of QOOH by dissociation or reaction is much faster than the isomerization back to RO_2, the key RO_2 → QOOH step is rate-limiting in cyclic ether production. Measurements of product formation in carefully controlled alkane oxidation[3] and some laser photolysis measurements[35] have been interpreted as fulfilling these conditions (equivalent to effective irreversibility of the isomerization step), which would enable rate coefficients for the isomerization to be derived from the measurements of cyclic ether or OH production. Supporting this view are measurements of radioactive products following the addition of ^{14}C-labeled butene to an *n*-butane oxidation system.[36] Labeled carbon was found only in those cyclic ethers generated from the initial QOOH isomer arising from HO_2 addition to the labeled butene. Rapid isomerization to the RO_2, and hence to other QOOH isomers, would result in ^{14}C labels appearing in other cyclic ethers; therefore, these results[36] have been taken as evidence that the reverse isomerization of QOOH to RO_2 is negligible.[9] However, these experiments cannot probe the range of QOOH radicals that are important in alkyl + O_2 reactions, and recent calculations[37−39] call into question whether the conditions for effective irreversibility of the RO_2 → QOOH isomerization are as easily attained as has been assumed.

Much of the progress in understanding the R + O_2 reaction systems has been obtained by measurements of product formation in alkane oxidation systems. Recently, the combination of state-of-the-art computational kinetics with experiments using pulsed-photolytic initiation of oxidation reactions has focused on increasing detail on the mechanism of these reactions. This article describes these measurements of product formation in pulsed-photolytic initiated hydrocarbon oxidation systems with an emphasis on the aspects of the reaction mechanism high-

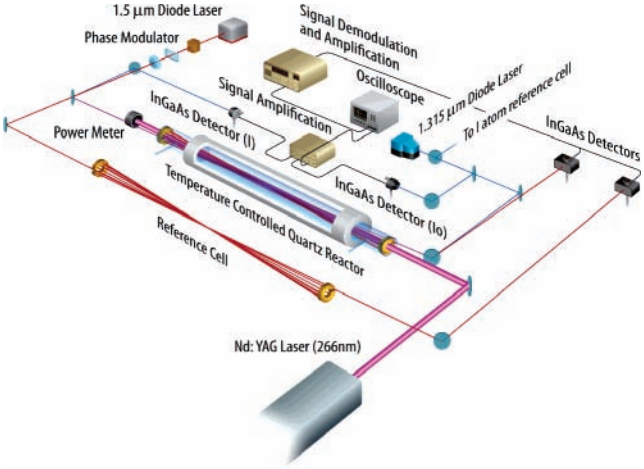

Figure 1. Typical experimental configuration for measurements of product formation in photolytically initiated oxidation reactions. The specific apparatus shown is that used in investigations of HO_2 formation in the reactions of alkyl radicals with molecular oxygen, initiated by photolysis of alkyl iodides. The laser wavelengths used may differ for other experiments, but the general features are similar.

lighted by comparison of the results to multiple-well time-dependent master equation calculations.

Experimental Methods

The experiments considered here have all employed pulsed laser photolysis to initiate oxidation chemistry and have followed the course of the subsequent reactions by either continuous-laser absorption measurements or, occasionally, pulsed laser-induced fluorescence. A typical experimental configuration is shown in Figure 1. The photolysis and probe lasers naturally differ for various initiation methods and reaction products, but the overall experimental method remains similar. Reactions take place in a slow-flow kinetic reactor, in which the gas flow is quasi-static on the time scale of the experiments but fast enough to replenish the reactor volume between photolysis laser shots.

Different initiation methods have been used to investigate the kinetics of product formation in alkyl + O_2 reactions. The Cl-initiated oxidation of alkanes is a straightforward way to investigate alkyl radical reactions with O_2. Chlorine atoms are produced by photolysis of a precursor such as Cl_2 or $CFCl_3$, and the Cl atoms react with an alkane, producing the alkyl radical and HCl, for example,

$$Cl + C_2H_6 \rightarrow HCl + C_2H_5 \quad (2)$$

The alkyl radical can then react with O_2:

$$C_2H_5 + O_2 \rightarrow \text{products} \quad (1)$$

This reaction scheme has several advantages for studying R + O_2 reactions. First, the abstraction of a hydrogen atom from an alkane by a Cl atom is nearly thermoneutral[40] and the alkyl radical is produced with negligible excitation above thermal energies. Second, the relative yield of HO_2, and, somewhat less reliably, OH, can be determined by use of the reference system of Cl-initiated methanol oxidation:

$$Cl + CH_3OH \rightarrow HCl + CH_2OH \quad (3)$$

$$CH_2OH + O_2 \rightarrow HO_2 + CH_2O \quad (4)$$

Concentrations of methanol and O_2 are set so that virtually all

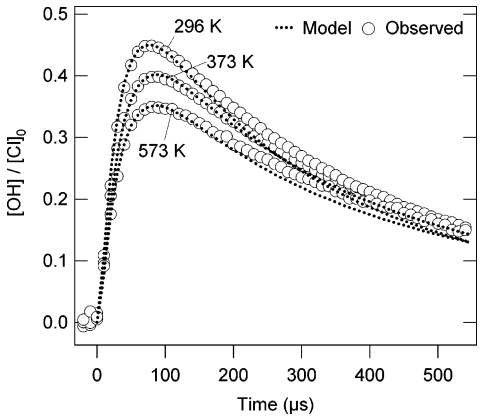

Figure 2. Hydroxyl radical absorption signals from the reference Cl_2/CH_3OH/O_2/NO reaction system, taken from the work of DeSain et al.[57] Note that the temperatures are mislabeled in the original figure. The model of the reference reactions is used to scale the observed OH absorption signal to the initial Cl atom concentration.

of the initially formed Cl atoms are rapidly converted HO_2. Under these conditions, the HO_2 signal rises rapidly and then decays according to a second-order rate law. The removal of HO_2 in the methanol system is dominated by the HO_2 + HO_2 reaction

$$HO_2 + HO_2 \rightarrow \text{products} \quad (5)$$

The reference reaction therefore also provides a measurement of the self-reaction of HO_2, which is another key advantage of the Cl-initiated oxidation scheme, as discussed below. The overall fractional conversion of initial Cl atoms to HO_2 in the Cl-initiated oxidation of the alkane can be readily determined by comparison of the HO_2 signal amplitude for alkane oxidation to the initial peak concentration measured for identical photolysis conditions in the methanol system.

The production of OH can be calibrated by modeling the methanol reference system with NO added, making use of the reaction

$$HO_2 + NO \rightarrow OH + NO_2 \quad (6)$$

to convert the HO_2 into OH. Implementation of this reference system as a calibration, however, requires kinetic modeling of the overall system because of the reactivity of the OH radical. This modeling, an example of which is shown in Figure 2, permits reporting the OH concentration as a fraction of the initial Cl concentration but naturally introduces additional uncertainties in the measurements of the overall fractional conversion of alkyl radicals to OH.

The Cl-initiated oxidation method also entails some significant disadvantages. First, Cl atom reactions with alkanes are not especially site-selective, and mixtures of isomers are formed in the oxidation of alkanes such as butanes or propane.[41] Second, the additional chemistry of the Cl atom precursor complicates the data analysis; for Cl_2 photolysis, the competition with chain chlorination requires that O_2 concentrations be relatively high, limiting the range of kinetic time scales.

Alkyl halide photolysis removes these disadvantages, and photolysis of halides has been widely employed to investigate alkyl reactions with O_2.[19,35,42−45] Alkyl iodide photolysis at 266 nm has been used to measure the HO_2 product formation from *i*-propyl and *n*-propyl radicals with oxygen.[29] The advantage of isomeric selectivity in the alkyl iodide photolysis must be weighed against the loss of the reference reaction used in the Cl-initiated oxidation method. Furthermore, although I atoms

are relatively unreactive, the side chemistry related to the I atom coproduct is not negligible. For this reason, and to gain a measure of the initial alkyl radical concentration, the time profile of the I atom is also measured in these experiments.

HO_2 Detection. The detection of HO_2 is accomplished by infrared two-tone frequency-modulation spectroscopy,[46−48] utilizing either the overtone of the O−H stretch[49] or the A−X electronic transition.[50] Frequency-modulation detection is valuable for the detection of transient absorption in photolytically induced experiments, both because of the reduction in laser amplitude noise as a consequence of moving the detection bandpass to higher frequency[51,52] and because of the vastly reduced sensitivity to thermal lensing noise, which is a consequence of the differential nature of FM signals.[53] Thermal lensing noise results from changes in the refractive index of the reaction mixture because of the transient heating following deposition of energy by the photolysis laser. This effect can often dominate the noise in a laser photolysis experiment.

A multipass cell[54] based on the Herriott[55] design is employed to increase the signal-to-noise ratio in the absorption and frequency-modulation measurements. This design sends the probe beam along an off-axis path in a spherical resonator; the probe traces a circle of spots on each mirror, and a smaller circle in the center of the cell, never actually touching the resonator axis. The photolysis laser is sent down the resonator axis, confining the overlap between pump and probe beams to the center of the cell, where the temperature can be regulated accurately. Typical path lengths are between 10 and 15 m, with from 21 to 35 passes of the probe beam through the reactor cell.

OH Detection. Because of the higher reactivity of the OH radical, its steady-state concentrations are much smaller than those of the relatively unreactive HO_2 radical. Moreover, the branching fractions to OH are much smaller than those to HO_2 in most R + O_2 reactions. As a result, detection of OH production often requires a more sensitive method than infrared absorption. In investigations of OH production in the oxidation of ethane, propane,[38,39] and neopentane,[56] laser-induced fluorescence detection was employed. However, for some reactions in which OH is a principal product, such as the reaction of cyclopropyl radical with O_2,[57] steady-state populations are sufficient to allow infrared absorption detection in the fundamental vibrational band.

Detection of I Atom. In experiments initiated by alkyl iodide photolysis, the time behavior of the I atom concentration is monitored by single-pass direct absorption of a diode laser probe tuned to the ($F' = 3$) ← ($F'' = 4$) hyperfine component of the ($^2P_{1/2}$ ← $^2P_{3/2}$) spin−orbit transition. The absorption strength of this transition is known,[58] and the absolute concentration of I atoms can therefore be determined. Under the assumption that every iodine atom is produced in conjunction with an alkyl radical, the initial I atom concentration will equal the initial alkyl radical concentration. However, for some alkyl iodides, sufficient energy remains in the alkyl radical following photolysis at 266 nm to produce some secondary dissociation, and the I atom concentration is an upper bound on the initial alkyl radical concentration. The time profile of the I atom concentration also provides a measure of the competing chemistry involving I atom reactions with HO_2 and RO_2 that must also be accounted for in the comparison of the experiments to theoretical models of the R + O_2 reactions.[29]

Approximate Methods for Data Inversion. In a series of time-resolved investigations of HO_2 production in Cl-initiated alkane oxidation,[26−28,37] inversion of the observed signals based on simplified kinetic models was used to extract an approximate overall production curve of HO_2 in the reaction system, as shown in Figure 3 for the case of Cl-initiated propane oxidation. Although this method has been partially superseded by the more accurate method of direct kinetic simulation,[29,38,39,56] the analytic correction of the observed HO_2 profile for the ongoing HO_2 self-reaction rigorously provides the minimum HO_2 production implied by the observed signal. This partially corrected concentration, $[HO_2]_t°$, is rigorously the minimum HO_2 production necessary to produce the observed signal, and it can be easily shown to be less than the concentration from a model that simply sets the self-reaction rate coefficient to zero. Mathematical details are given as Supporting Information.

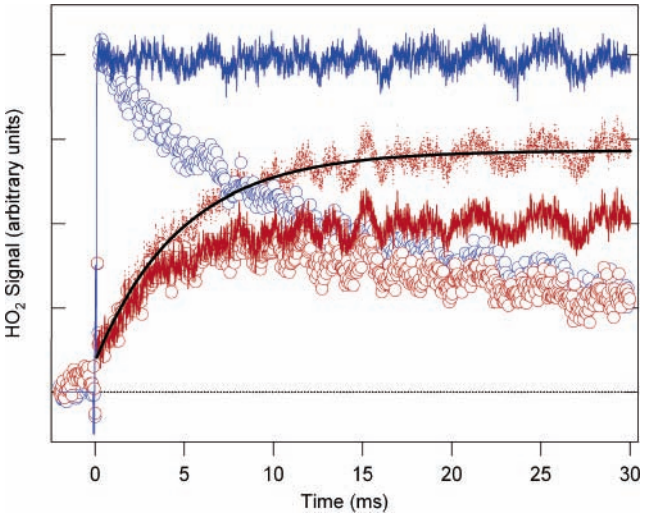

Figure 3. Approximate method of data inversion to extract the HO_2 production curve from the observed HO_2 signal. The blue circles show the raw signal from the reference reaction of Cl-initiated methanol oxidation, which quantitatively converts the initial Cl atom concentration to HO_2. The red circles show the raw signal from Cl-initiated propane oxidation under the same Cl_2 photolysis conditions.[26] Partial correction of the signals for the effects of HO_2 self-reaction yields the solid traces. The approximate correction of the Cl-initiated propane oxidation measurement for reactions of RO_2 with HO_2 results in the trace shown as the red dots. A fit to these data, represented by the solid black line, gives the HO_2 yields and effective rate constants for formation.

In several publications,[26−28,37] this method was extended to further correct the signals for the contributions of other removal reactions of HO_2. This approach is by its nature approximate, as the full chemistry of the Cl-initiated oxidation system is considerably more complex than can be described in a straightforwardly invertible form. The central assumptions are that all initially formed alkyl radicals produce either alkylperoxy radicals or HO_2 and that the equilibrium for the R + O_2 addition greatly favors the RO_2 products. Where substantial OH production occurs in the R + O_2 reaction, the simplification is expected to dramatically fail, as was noted for the cases of butyl,[37] cyclopropyl,[57] and neopentyl[56] radical oxidation. However, this approximate inversion of the kinetics generates an experimentally based curve of HO_2 production, depicted as the dots in Figure 3, that can be analyzed to give values for HO_2 yield and effective HO_2 formation rates. These yields and formation rates cannot be assigned simply as branching fractions or rate coefficients of the R + O_2 reaction but are effective quantities for the overall oxidation system and will depend on secondary reactions, side reactions, and conditions such as overall radical densities. This distinction was made in the first paper where this method was applied[27] and emphasized in later papers.[26,28,37] Even with these substantial caveats, the "fully corrected" yield

often appears to be a reasonable approximation to the result of a full kinetic simulation.[29,59]

Comparison of Experiment and Detailed Theory. As rigorous parametrizations of time-dependent multiple-well master equation results have become available,[60] it is now clear that full modeling of the kinetics is a more reliable approach than approximate data inversion. Moreover, no inversion scheme is practical for measurements of the OH radical, and OH production is tied to the critically important isomerization to QOOH. Therefore, the present strategy has been developed, which uses the comparison of experimental measurements with high-level computational kinetics results to infer adjustments (within the estimated uncertainty of the quantum chemical calculations) to ab initio energies of stationary points on the potential energy surface. The kinetic parameters are computed from full time-dependent multiple-well Rice−Ramsperger−Kassel−Marcus (RRKM) master equation solutions,[5,6,61−64] using variable-reaction-coordinate variational transition-state theory[65−68] for channels without a well-defined saddle point. More qualitative or more semiempirical kinetic treatments, such as quantum Rice−Ramsperger−Kassel (QRRK) or modified strong-collision models, can provide useful parametrizations of R + O_2 reactions and are valuable for certain modeling applications, or where rapid approximate evaluation of rate coefficients is necessary.[59,69−73] However, these methods are not rigorous enough to reliably extract information on stationary point energies from comparison to experiments.

One of the key features that arises from the decomposition of the multiple-well time-resolved master equation results into rate coefficients is the necessity of including rate coefficients for formally direct reactions across several transition states. A simple example is the direct formation of HO_2 from the R + O_2 reactants via the chemically activated RO_2 radical. The reactants traverse the entrance transition state between reactants and the RO_2 well and the transition state for elimination of HO_2 from the RO_2 radical. This process is nevertheless direct; the chemically activated RO_2 species dissociates to products before stabilization, and the reaction is modeled as a single kinetic step. In many hydrocarbon oxidation models, such processes are described as sequential elementary steps across the individual transition states, for example, the formation of OH + methyloxirane from *i*-propyl + O_2 is modeled as the formation of the *i*-propylperoxy radical from the reactants, followed by isomerization to a 2-hydroperoxypropyl radical, followed by dissociation and ring closure to form the OH and methyloxirane products. As will be shown below, such a sequential modeling scheme significantly fails to capture the time-resolved experimental observations.

The kinetic parameters calculated using the adjusted stationary point energies constitute the fitted model of the R + O_2 reaction. The various phenomenological rate coefficients in the model of an individual R + O_2 reaction are related to one another through the topography of the relevant potential energy surface. For example, the rate coefficient that governs the chemically activated formation of HO_2 from ethyl + O_2 is related to the rate coefficient for thermal elimination of HO_2 from the ethylperoxy radical, because the two processes share a transition state. Modeling the reaction by modification of stationary point energies and recalculation of the phenomenological rate coefficients ensures that this set of rate coefficients remains internally consistent, an assurance that is not necessarily available from an independent fit of rate coefficients to experiment.

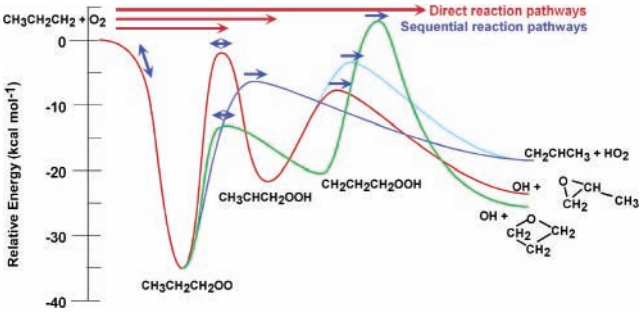

Figure 4. Schematic depiction of the potential energy surface for the reaction of *n*-propyl radicals with molecular oxygen. The stationary point energies are those calculated in ref 37. Time-dependent master equation modeling yields values for all rate coefficients in the system, both for sequential pathways (conceptually, those traversing a single transition state) and for direct chemically activated pathways that traverse multiple transition states.

Fundamental Characteristics of Alkyl + O_2 Reactions

The mechanism of the general alkyl + O_2 reaction can be visualized by considering the schematic potential energy surface of the simplest truly prototypical R + O_2 reaction, that of *n*-propyl with O_2. A representation of the relevant stationary point energies[37] is given in Figure 4, as calculated using a composite method "HL2" employing QCISD(T) calculations with a 6-311G(d,p) basis set and an MP2 basis-set correction to approximate QCISD(T)/6-311++G(3df,2pd) energies:

$$E_{HL2} = E[\text{QCISD(T)/6-311G(d,p)}] + E[\text{MP2/6-311++G(3df,2pd)}] - E[\text{MP2/6-311G(d,p)}] \quad (7)$$

At this level, the $CH_3CH_2CH_2O_2$ radical is calculated to be bound by 34.9 kcal mol^{-1} and has two accessible internal isomerization pathways: to CH_3CHCH_2OOH via a five-membered ring transition state lying 2.6 kcal mol^{-1} below the energy of the reactants and to $CH_2CH_2CH_2OOH$ via a six-membered ring transition state lying 11.2 kcal mol^{-1} below the energy of the reactants. The $CH_3CH_2CH_2O_2$ radical can also form HO_2 and propene by direct elimination over a transition state calculated to be 5.2 kcal mol^{-1} below the reactants' energy. Whereas the CH_3CHCH_2OOH radical can readily form HO_2 or OH radicals by dissociation through transition states lying below the energy of *n*-propyl + O_2, the dissociation channels of the $CH_2CH_2CH_2OOH$ radical have transition states well above the reactants' energy.

The earlier controversy concerning the possibility of a "parallel mechanism" in which HO_2 formation proceeded by direct abstraction rather than via the RO_2 intermediate has been settled in favor of the coupled mechanism, in which all products are related to the initial alkylperoxy complex. The measurements of product formation following photolytic initiation therefore reflect the competition among stabilization, dissociation, and isomerization of the RO_2 species.

Stabilization of RO_2. The presence of the relatively deep RO_2 well permits the dominance of stabilization to alkyl peroxy radicals at low temperatures and high pressures and affects the behavior of the reaction at temperatures through the transition region. In Figure 5, the HO_2 formation from the Cl-initiated oxidation of ethane is displayed for two temperatures. At the lower temperature (423 K), the HO_2 is formed directly from the chemically activated RO_2 radical, before it can be collisionally stabilized. Under the conditions of these experiments, thermal decomposition of stabilized RO_2 radicals is too slow

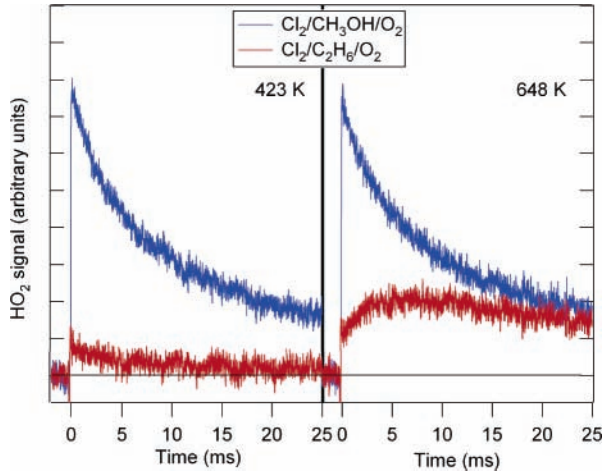

Figure 5. Measurements of HO_2 formed by Cl-initiated oxidation of ethane at two temperatures.[27] The blue traces are HO_2 formed by the reference reaction system of Cl-initiated methanol oxidation, which transfers the initial Cl atom concentration quantitatively into HO_2. The red traces are HO_2 formed from the Cl-initiated oxidation of ethane. At low temperatures, prompt formation via the direct, chemically activated pathway is the only significant means of HO_2 production. At higher temperatures, however, secondary production via thermal dissociation of the alkylperoxy radical begins to dominate.

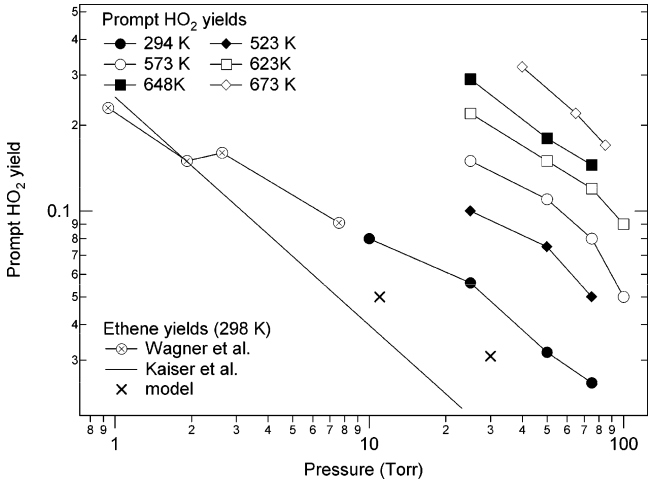

Figure 6. Prompt yields of HO_2 from the reaction of C_2H_5 with O_2, as a function of pressure and temperature.[27] Also shown are the total yield of ethene at 298 K, as measured by Wagner et al.,[19] and the fit to the pressure-dependent ethane yield data of Kaiser and co-workers.[12,14] The total yield of HO_2 + ethene in the model of DeSain et al.[38,39] is shown as the crosses.

to compete with reactive removal of the RO_2 radicals, and the alkylperoxy radical channel is effectively irreversible. As a result, the observed HO_2 signal rises rapidly, within the rise time of the frequency-modulation apparatus for the propane and oxygen concentrations used here, and subsequently smoothly decays away. An apparent yield of HO_2 in this case can be defined by a simple ratio of the amplitudes of the initial rises of the alkane oxidation signal and the reference methanol signal. In a series of circumspect continuous-photolysis chlorine-initiated oxidation experiments, Kaiser and co-workers[12,14,30,74,75] have shown a power-law dependence of the alkene yield on total pressure, p, over a wide pressure range for both ethyl + O_2 and propyl + O_2. The time-resolved measurements of ethene[19] and HO_2 formation[26,27] at low temperatures corroborate this picture, with decreasing yields as pressure increases, as shown in Figure 6, although there is an interesting discrepancy[59] between the time-resolved experiments[19,27] and the continuous-photolysis experiments[12,14] for ethane oxidation at room temperature. Reference to an HO_2 or RO_2 branching fraction generally entails some assumption on the time scale of the experiment or on the subsequent chemistry removing RO_2,[27] because the formation of RO_2 is essentially reversible for many experimental conditions. At room temperature, HO_2 and ethene are formed almost exclusively via the direct chemically activated pathway, and the time scale of HO_2 formation is too short for most competing radical−radical reactions, which could reduce the apparent HO_2 yield, to be significant. Nevertheless, it should be borne in mind that all of the available measurements are subject to secondary and side chemistry,[27,59] and modeling of the entire reaction system may be necessary to accurately correlate experiments with models.[38,39] These considerations become more important as the temperature increases.

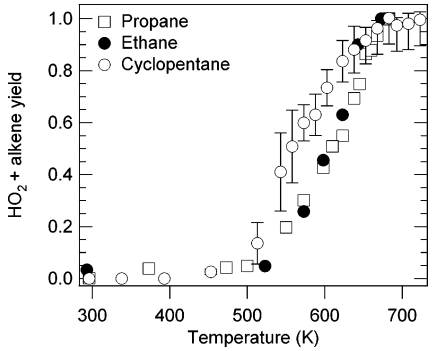

Figure 7. Observed overall yields of HO_2 in Cl-initiated oxidation of ethane[27] (filled circles), propane[26] (open squares), and cyclopentane[28] (open circles) as a function of temperature. Representative uncertainties are shown for the cyclopentane data. At temperatures where the dissociation of the RO_2 radical begins to dominate over removal by radical−radical reactions, the yield of bimolecular products in the R + O_2 reaction increases sharply. Experiments at lower total radical density (and hence smaller rates of RO_2 removal by radical−radical reactions) show this sharp increase at lower temperatures.[14,30,75]

At higher temperatures, the dissociation of the alkyl peroxy radical becomes more rapid, and this thermal dissociation reduces the yield of stabilized RO_2 products and hence increases the overall yield of all bimolecular products, including HO_2 + alkene. As shown in the right panel of Figure 5, the HO_2 production displays two clear time scales; a delayed production of HO_2 is visible after the prompt rise in HO_2. The prompt rise, as at lower temperatures, is due to the direct formation of HO_2 from the R + O_2 reactants, via the chemically activated RO_2. The longer-time HO_2 production reflects the dissociation of RO_2 radicals, both directly to HO_2 + alkene and back to alkyl radical reactants. The overall yield of HO_2 increases dramatically as the alkylperoxy radical becomes thermally unstable. Figure 7 displays this overall yield, extracted via the approximate inversion procedure, for several Cl-initiated alkane oxidation systems. The uncertainty in the overall yields from this procedure is estimated to be about ±10%; recent comparison with detailed kinetic modeling of the ethyl + O_2 system finds yields approximately 10% higher than those extracted by the data inversion procedure.[59] Kaiser[14,30,75] measured alkene yields as a function of temperature in continuous-photolysis Cl-initiated alkane oxidation reactions and found similar behavior but observed the increase in alkene yield at 50 K to 100 K lower temperature than in the HO_2 yield measurements. The temperature at which the yield of bimolecular products increases is the point at which the dissociation of RO_2, either to HO_2 + alkene or back to reactants, is rapid enough to overcome the other removal reactions for RO_2 in the system. The Kaiser experiments are carried out at a far lower total radical density

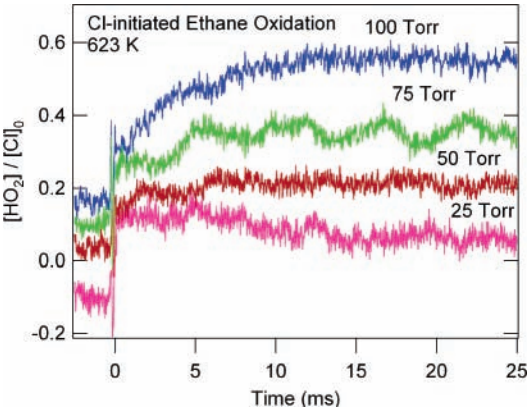

Figure 8. Measurements of HO_2 concentration in Cl-initiated ethane oxidation at 623 K, taken at several pressures.[27] The traces are normalized to the initial Cl atom concentration and are shifted vertically for clarity. The prompt HO_2, given by the initial rise of the signal, decreases with increasing pressure; the secondary, delayed formation of HO_2 increases with increasing pressure.

than the pulsed-photolytic measurements of HO_2 production. Because the dominant bimolecular removal reactions of RO_2 are radical−radical reactions, this higher radical density requires the unimolecular dissociation of RO_2 to reach a larger rate in the pulsed-photolytic experiments before it dominates RO_2 removal. The difference in radical density quantitatively describes the temperature shift of the rise in bimolecular product yield between the two sets of experiments.[27,29,30] Kaiser[30] has also analyzed the branching of RO_2 dissociation by comparing C_2H_4 yields to the C_2H_5Cl produced by side reactions of ethyl with the molecular chlorine photolyte. His work suggests a substantial role for thermal formation of $HO_2 + C_2H_4$ directly from the ethylperoxy radical.

The effects of stabilization into the RO_2 well continue to be discernible in the HO_2 formation at elevated temperature. The fraction of HO_2 that is produced in the direct pathway continues to decrease with increasing pressure at higher temperatures, as shown for ethyl + O_2 in Figure 6. The negative pressure dependence of the prompt yield persists even at temperatures where the total HO_2 yield is approximately unity and has a negligible pressure dependence. As can be seen from Figure 8, in which HO_2 production from Cl-initiated ethane oxidation at 658 K is displayed for three different total pressures, the decrease in the amplitude of the prompt HO_2 is counteracted by an increase in the amplitude of the secondary formation of HO_2. The traces have been normalized to the initial Cl atom concentration by comparison to the methanol reference reaction. The rate coefficients for the addition-stabilization reaction to form ethylperoxy and the unimolecular dissociation of ethylperoxy to HO_2 and ethene are increasing with pressure under these conditions. Nevertheless, the pressure dependence of the time constant for the secondary formation of HO_2 (as obtained from exponential fits to the HO_2 production profiles obtained by the approximate inversion procedure) is slight.[26−28] Modeling the time behavior of the HO_2 concentration in the transition region is sensitive to both the transition state for HO_2 elimination and the RO_2 well depth.

Direct Elimination of HO_2. Figure 9 displays the results of such a model, for the reactions of the *n*-propyl radical with O_2 and the *i*-propyl radical with O_2.[29] These reactions are initiated by photolysis of the corresponding iodides, and the measured I atom absorptions are shown as insets. The kinetic model for each of these oxidation systems includes more than 50 reactions, but the rise of the HO_2 signal is most sensitive to the R + O_2

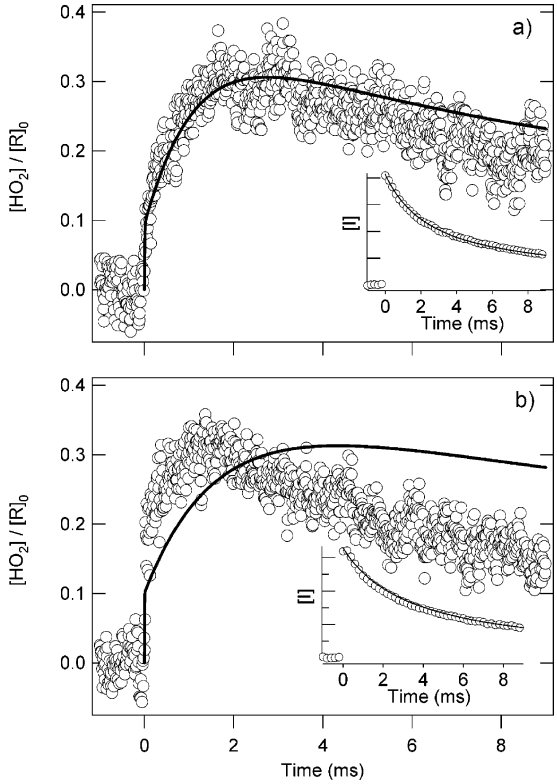

Figure 9. Measurements and modeling of the formation of HO_2 in the reaction of (a) *n*-propyl radicals and (b) *i*-propyl radicals with oxygen at 673 K. The experimental data are given as the open circles (only every 10th point is shown for clarity), and the kinetic model is displayed as the solid black lines. The reactions are initiated by photolysis of the suitable propyl iodide; the measured (only every 200th point is displayed) and modeled relative I atom concentrations are shown in the insets.

reaction mechanism and reactions of HO_2 and RO_2 with each other and with I atoms. In the model for the *n*-propyl + O_2 reaction, the transition state for elimination of HO_2 from $CH_3CH_2CH_2OO$ is raised by 1.4 kcal mol^{-1} from the ab initio value, and the transition state for isomerization from $CH_3CH_2CH_2OO$ to CH_3CHCH_2OOH is also raised by 0.5 kcal mol^{-1}, to achieve the best agreement with the body of experimental data, including literature measurements. Other stationary point energies are unchanged from the ab initio values.[37] As can be seen from Figure 9, the agreement between theory and experiment that is generated by these adjustments is outstanding. Similar agreement is obtained for HO_2 formation in ethyl + O_2 reactions.[29]

In a similar way, the $(CH_3)_2CHOO$ well depth has been decreased by 0.6 kcal mol^{-1} from the ab initio value, to 36.2 kcal mol^{-1}, and the transition state for HO_2 elimination has been raised by 2 kcal mol^{-1} from the ab initio value, to 5 kcal mol^{-1} below the energy of the reactants. The transition state for isomerization from $(CH_3)_2CHOO$ to $CH_3CH(CH_2)OOH$ has been raised by 2.3 kcal mol^{-1}, principally to better model OH production.[38,39] As shown in Figure 9, these changes produce modest agreement with the HO_2 formation measurements. Adjustment is further constrained by literature measurements of the equilibrium constant for the addition of *i*-propyl to O_2[76] and of the high-temperature rate coefficient for *i*-propyl + O_2 derived by Gulati and Walker.[16] A model in which the elimination transition state of HO_2 from *i*-$C_3H_7O_2$ is raised by only 1 kcal mol^{-1} and the *i*-$C_3H_7O_2$ well depth remains unchanged from the ab initio calculation will reproduce the experimental HO_2 profiles with a similar accuracy to that of

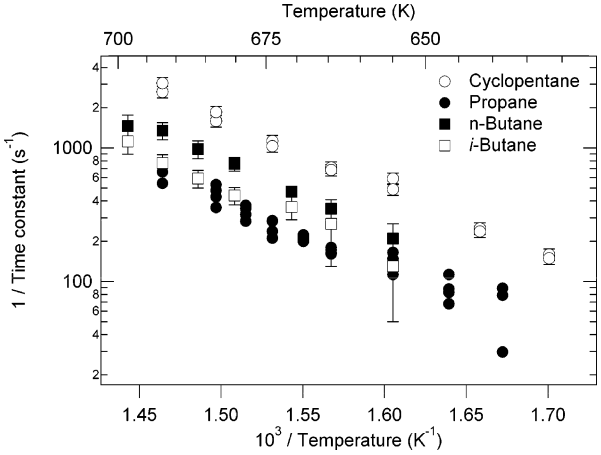

Figure 10. Arrhenius plot of the effective rate coefficient for the secondary formation of HO_2 from RO_2 dissociation, measured in Cl-initiated alkane oxidation.[26,28,37] Although this quantity is not an elementary rate coefficient, the similarities in the apparent activation energies across various alkane systems reflect similar energetics of the HO_2 elimination from the RO_2 radical. The larger effective rate coefficient for the cyclopentane oxidation is attributed to the lack of free rotation about the C−C bonds of the RO_2 radical.[28]

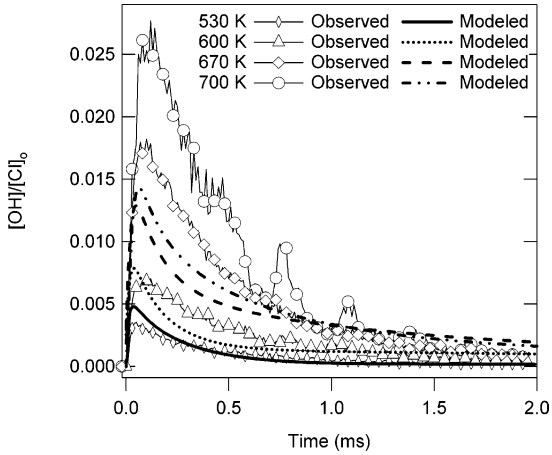

Figure 11. Measured and modeled OH concentrations in the Cl-initiated oxidation of propane.[38,39] Symbols are placed only on every fifth data point for clarity.

the *n*-propyl model. However, the agreement with these literature measurements is diminished. This discrepancy is being investigated further by measurements of deuterated *i*-propyl radical reactions with O_2,[77] which probes the same potential energy surface; a reinvestigation of the high-temperature kinetics of the $i\text{-}C_3H_7 + O_2$ reaction may be useful. Nevertheless, the present "compromise" model of the $i\text{-}C_3H_7O_2$ system produces reasonable agreement with the body of available data.

The comparison of experimental HO_2 profiles to computational kinetics models results in an experimentally validated set of elementary rate coefficients that can reproduce the master equation results. However, these detailed investigations are so far limited to the smallest alkyl + O_2 systems. Even as calculations of larger systems become feasible, it will remain impractical to perform full multiple-well time-resolved master equation analysis with high-level quantum chemistry for every chemically activated reaction in combustion. Extension of the detailed small-radical models to larger systems will require general rules for individual rate coefficients and empirical correlations of phenomenological measurements such as product yields and effective rate coefficients. Comparison of the approximate secondary HO_2 production rate constants in the oxidation of several alkanes provides qualitative correlations that may aid in more general semiempirical estimates of HO_2 formation in larger alkanes. Figure 10 shows this effective rate constant as a function of temperature for butane,[37] propane,[26] and cyclopentane[28] oxidation. Recall that this effective rate coefficient is not a rate constant for an elementary kinetic step but reflects a convolution of reaction, stabilization, and dissociation of the RO_2 radical. The apparent activation energy for this secondary formation is similar for all of the alkane oxidation processes in which it has been measured,[26−28,37] reflecting in part similar energetics of the HO_2 elimination transition state. In fact, the secondary HO_2 production in Cl-initiated butane oxidation[37] can be predicted by a relatively simple extension of the validated master equation results for propane oxidation.

The effective rate coefficient for secondary HO_2 formation in cyclopentane oxidation is larger than those for the other alkane oxidations that have been measured, approximately 4 times as great as that in propane oxidation. This difference can be rationalized by the expected difference in the enthalpy of activation for the HO_2 elimination from the propylperoxy and cyclopentylperoxy radicals. The elimination proceeds via a five-membered ring (H−C−C−O−O) transition state in both molecules. In either propylperoxy radical, free rotation around a carbon−carbon single bond in the reactant is lost upon going to the transition state. In the cyclopentylperoxy radical, there is no free rotation about the C−C bonds, so the difference in entropy between the reactants and the transition state will be smaller, and the A-factor therefore larger. The approximate factor of 4 increase is broadly consistent with that expected on the basis of the entropy of a methyl rotor. This increase in the A-factor for HO_2 elimination should be common to alkylperoxy species formed from cyclic hydrocarbon radicals.

Isomerization and Formation of OH. The elimination of HO_2 from the alkylperoxy radicals is the principal reaction pathway for the R + O_2 reactions at temperatures above the transition region. Because of the low reactivity of the HO_2 radical, this pathway is essentially chain-terminating until even higher temperatures, when dissociation of hydrogen peroxide (the product of reactions of HO_2) is rapid enough to sustain the chain reaction. Chain branching at lower temperatures occurs by reactions of the hydroperoxyalkyl radicals (QOOH) that result from isomerization of the alkylperoxy radicals. This isomerization competes with the formation of HO_2 and also produces OH radicals and cyclic ethers. Measurement of the OH products of the R + O_2 reactions is therefore related to key processes of chain branching in low-temperature hydrocarbon oxidation.

Determination of time-resolved OH production from the R + O_2 reactions in which it is a minor product is a particular experimental challenge. Figure 11 shows laser-induced fluorescence measurements of OH concentrations in Cl-initiated oxidation of propane.[38,39] In these experiments, the photolytic precursor is CCl_3F, chosen in order to avoid high-temperature chain reactions that occur in the $Cl_2/CH_3OH/O_2/NO$ reference system. The observed OH signals have been modeled by a kinetic mechanism that includes removal reactions of the OH radical as well as side and secondary reactions. These results are shown as the lines in Figure 11. The agreement between the model and the experiment is qualitatively good; furthermore, the model predicts larger OH production from propane oxidation than from ethane oxidation, in accord with experiment. The contribution of formally direct channels for OH production from alkyl + O_2, via chemically activated alkylperoxy radicals, is especially important in modeling OH production in the Cl-

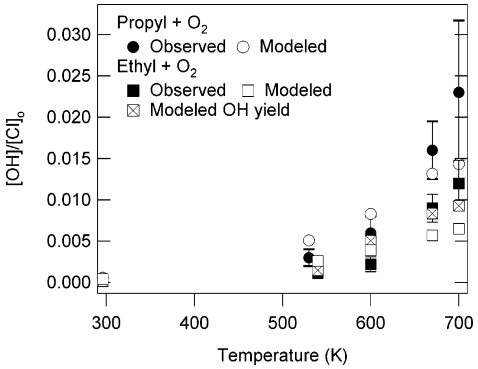

Figure 12. Measured (solid symbols) and modeled (open symbols) peak OH concentrations, relative to the initial Cl atom concentration, in the Cl-initiated oxidation of ethane (squares) and propane (circles). The modeled overall yield of OH in the ethyl + O_2 reaction is shown as the crossed squares for reference; the peak concentration is not expected to be the same as the overall yield.

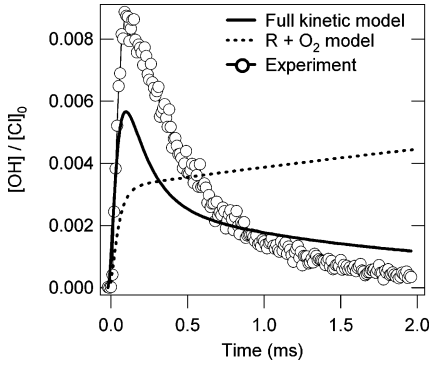

Figure 13. Measurements and modeling of the production of OH from the ethyl + O_2 reaction. The open circles are from laser-induced fluorescence measurements of OH from Cl-initiated oxidation of ethane at 670 K, normalized to the initial Cl atom concentration.[38,39] The solid line represents the predicted OH concentration from a kinetic model that accounts for side and secondary reactions. The dotted line shows the integrated production of OH from the reaction of ethyl + O_2 as used in the full kinetic model. Significant production of OH continues well after the observed peak in OH concentration. The modeled overall yield of OH in the ethyl + O_2 reaction under these conditions is 0.0084.

initiated oxidation systems. Because of the high reaction rate of OH with the large excess of alkane, significant OH concentrations are built up only for relatively rapid OH production, as occurs by direct reaction soon after the photolysis pulse.

However, clearly, the agreement between the model and the experiment is not as good as in the case of the HO_2 production. The model predicts too much OH at low temperature and too little OH at high temperature, as displayed in Figure 12 for ethane and propane oxidation. This lack of agreement is disappointing for the product most clearly related to the chain branching path in the R + O_2 reactions. Several possible sources of the discrepancy can be proposed. First, one can imagine that the stationary point energies could be further adjusted. However, the models are constrained not only by the time-resolved OH studies but also by the HO_2 measurements,[26,27,37] the kinetics and equilibrium constant determinations of Knyazev, Slagle, Gutman, and co-workers,[19,20,45,76] and the end-product measurements of Kaiser[12−14,30,74,75] and Walker[3,15,16,18,22,23,78] and their co-workers. Second, reactions of the QOOH species with O_2 can produce OH. Calculations of stationary point energies for these reactions are becoming available.[79,80] On the basis of the results of Bozzelli and Sheng[79] on the $C_2H_4OOH + O_2$ reaction, it is estimated that direct reactions of QOOH with O_2 to form OH could increase the modeled peak OH concentration by up to 20%, bringing the model closer to the measurement.[38,39] Full multiple-well time-dependent master equation calculations may elucidate the possible role of these reactions in forming OH in these systems. Finally, the kinetic mechanism for modeling OH concentrations is affected by several reactions whose rate coefficients are somewhat poorly characterized, especially the reactions of HO_2 with alkyl radicals or the CCl_2F photolysis coproduct, both of which can produce OH radicals.

Carstensen and co-workers[59] have matched the measured peak OH concentration measurements[38,39] to their total modeled OH yield for the ethyl + O_2 reaction. This tactic provides a closer apparent match between the model and the experimental data (see Figure 12) but is a scientifically untenable method of data analysis. The high reactivity of the OH radical precludes such a simple correlation of concentration with production, and much of the OH production occurs after the peak in the observed concentration is reached, as is shown in Figure 13. The effects of side and secondary chemistry on the observed OH signal are vastly greater than in the case of HO_2, for which there is general agreement[27,59] that modeling is necessary to relate signals to product yields. The difference between the temperature dependence of the modeled overall OH yield and that of the peak OH concentration underlines the need for closer investigation of the other reactions in the kinetic model, especially the reactions of alkyl radicals with HO_2.[38,39] The peak in the modeled OH concentration is dominated by the prompt yield and side chemistry involving HO_2; the longer-term OH production gives a much smaller steady-state concentration. The difficulties with accounting for the side chemistry suggest that different photolysis systems (with different side and secondary chemistry) should be used to further investigate OH formation. Some such experiments, employing ultraviolet absorption probing following alkyl halide photolysis or photolysis of different Cl atom precursors, are currently underway in the author's laboratory.

Rate coefficients for $RO_2 \rightarrow$ QOOH isomerization have been derived on the basis of the extensive measurements of Walker and co-workers[3] of cyclic ether formation relative to alkene formation for a wide variety of R + O_2 systems. These relative measurements have been anchored by the OH formation measurements of Hughes et al.[35,42] The reaction of neopentyl radicals with O_2 focuses on the isomerization of RO_2 to QOOH, because the competing pathway of direct elimination of HO_2 is impossible, as neopentyl has no conjugate alkene. In the analysis of these experiments, it has been assumed that the dissociation of the hydroperoxyalkyl radicals and the reaction of the QOOH species with oxygen were significantly more rapid than the isomerization of QOOH back to the RO_2 radical,[3,4,81−85] so that the forward reaction of RO_2 to QOOH could be treated as essentially irreversible. Hughes et al.[35,42] derived a rate coefficient for neopentylperoxy isomerization to hydroperoxyneopentyl of approximately 1200 s^{-1} at 700 K. However, the analogous isomerization in *n*-propylperoxy, to $CH_2CH_2CH_2OOH$ via a six-membered ring transition state, is calculated to be almost 20 times faster.[38,39] This large of a discrepancy between two closely analogous systems would be extremely surprising. If the isomerization rate constant for neopentylperoxy were much faster than that reported by Hughes et al., it could have significant consequences for modeling of ignition chemistry, because of the position of the neopentylperoxy measurements as a benchmark for $RO_2 \leftrightarrow$ QOOH isomerizations.[3,4]

Time-resolved measurements of OH production in the Cl-initiated oxidation of neopentane are shown in Figure 14. Partly because of the complexity of the neopentyl + O_2 system and partly to explore the extension of validated models of simple R

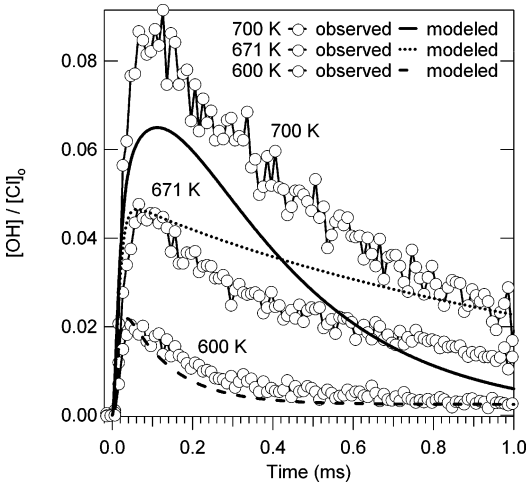

Figure 14. Measured OH concentrations from Cl-initiated oxidation of neopentane, normalized to the initial Cl atom concentration.[56] The modeled concentration uses an ad hoc extension of the validated model of *n*-propyl + O_2 to predict rate coefficients in the neopentyl + O_2 reaction.

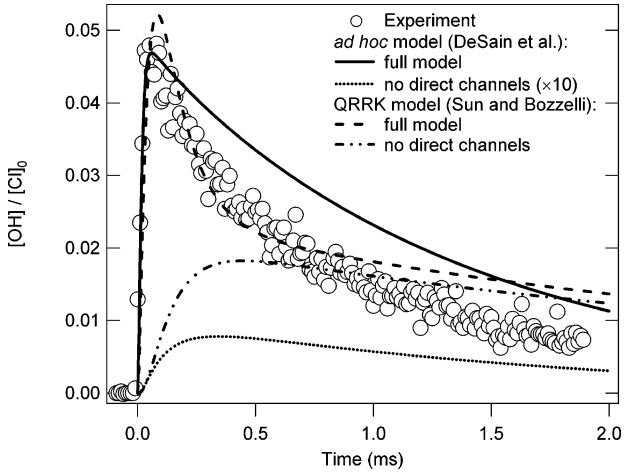

Figure 15. Measured OH concentration from Cl-initiated oxidation of neopentane at 671 K, normalized to the initial Cl atom concentration.[56] The solid line gives the modeled concentration using an ad hoc extension of the validated model of *n*-propyl + O_2 to predict rate coefficients in the neopentyl + O_2 reaction; the dotted line shows the results of this model without contributions from direct chemically activated formation of OH from neopentyl + O_2. The dashed line shows the results of the same model, but with the rate coefficients for OH formation taken from the calculations of Sun and Bozzelli.[80] The dot−dashed line represents the output of this modified model without the chemical activation contributions estimated by Sun and Bozzelli.[80]

+ O_2 reactions to larger systems, an ad hoc model is constructed by analogy to the *n*-propyl + O_2 system,[56] in place of a full master equation calculation. The A-factors for the neopentylperoxy isomerization to hydroperoxyneopentyl and for the direct formation of OH + 3,3-dimethyloxetane from neopentyl + O_2 are increased by a factor of 3 over those for the analogous processes in *n*-propyl + O_2 to account for the larger number of hydrogen atoms available to participate in the neopentylperoxy isomerization. The activation energies are taken to be those of the validated analogous *n*-propyl processes, changed by the *difference* between the relevant transition-state energies in the two systems, calculated at low-level density-functional theory (B3LYP/6-31G*). The equilibrium constant for neopentylperoxy formation from neopentyl + O_2 is changed by a factor of 5 from the *n*-propyl + O_2 system, bringing it into close agreement with the equilibrium constant employed by Hughes et al.[35,42] Finally, the rate constant for direct OH formation is arbitrarily increased by an additional factor of 3.[56] The results of this ad hoc model, when placed into a full kinetic simulation, simulate the OH measurements well over a wide temperature range. The contribution to the observed signal of reactions of alkyl radicals and $CFCl_2$ radicals with HO_2 is much smaller in the neopentane oxidation than in ethane or propane oxidation because the lack of direct HO_2 production in the neopentyl + O_2 reaction results in much smaller HO_2 concentrations in the first few hundred microseconds after photolysis.

The ad hoc model for neopentane oxidation now includes a rate coefficient for neopentylperoxy isomerization to hydroperoxyneopentyl that is 60 times that derived by Hughes et al.[35,42] A similarly constructed ad hoc model can reproduce all of the experimental observations of Hughes et al.,[35,42] as well as the more recent measurements,[56] suggesting that the isomerization could be easily reversible in the earlier observations and that the available experiments do not directly probe the rate of the isomerization. Recently, Sun and Bozzelli[80] have performed higher-level calculations of stationary point energies in the neopentyl + O_2 and hydroperoxyneopentyl radical + O_2 reactions and have carried out simple kinetics computations on both systems. Their calculations include a chemical activation analysis to estimate rate coefficients of formally direct pathways[80] and predict a rapidly equilibrating $RO_2 \leftrightarrow$ QOOH isomerization, with forward rate coefficients computed to be about 3 times as large as those of Hughes et al.[35,42] (approximately 3800 s^{-1} at 700 K) but substantially smaller than those in the ad hoc model based on *n*-propyl master equation results. Figure 15 shows the result of using the Sun and Bozzelli calculations for the $RO_2 \leftrightarrow$ QOOH isomerization and for the dissociation of QOOH to OH + 3,3-dimethyloxetane in the kinetic model for OH formation from Cl-initiated neopentane isomerization, compared to the experimental results at 673 K. The agreement is relatively good, raising hopes that comparison of experimental data with more rigorous kinetic calculations using computed stationary point characteristics will provide validated model rate coefficients for this key alkyl + O_2 system.

It is clear that new experiments must be developed if the $RO_2 \rightarrow$ QOOH isomerization rate is to be probed directly. Measurements with labeled reagents, carried out under different temperatures, pressures, and oxygen concentrations for various small and large hydrocarbon radicals, may prove extremely valuable. Previous measurements of cyclic ether production following HO_2 addition to labeled alkenes[36] unavoidably produce only those QOOH radicals with the radical site on the carbon next to the carbon attached to the oxygen. These radicals, which isomerize to RO_2 through a five-membered ring transition state, have barriers to isomerization that lie well above the barriers to OH or HO_2 formation,[37] so dissociation readily competes with isomerization. However, the isomerization via a six-membered ring transition state has a low activation energy but relatively high-energy transition states for OH or HO_2 formation.[37−39,56] As a result, this type of $RO_2 \leftrightarrow$ QOOH isomerization is particularly unlikely to be effectively irreversible under normal conditions.[86] Determining the range of conditions under which the isomerization is effectively irreversible and the formation of cyclic ether products can be taken as a reliable indicator for the isomerization may allow the parametrization of $RO_2 \rightarrow$ QOOH isomerization rate coefficients[3] to be redefined, as necessary, in a rigorous manner.

Formally Direct Pathways in Kinetic Models. The kinetic signature of the formally direct pathway from the reactants to the HO_2 product is unmistakable: the prompt rise in the HO_2 signal. In the case of OH formation, the signature is less striking

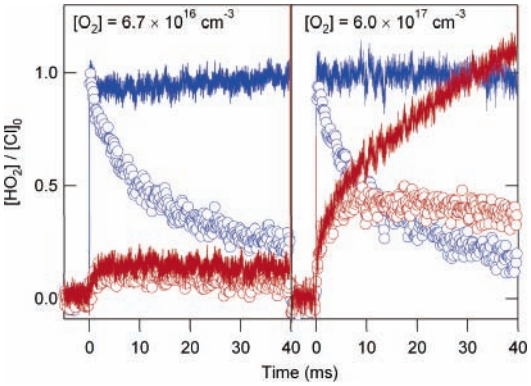

Figure 16. Measurements of HO_2 in the Cl-initiated oxidation of neopentane, normalized to the initial Cl atom concentration.[56] The reference system of Cl-initiated methanol oxidation, which quantitatively transfers the initial Cl atom concentration to HO_2, is shown in blue, and the Cl-initiated neopentane oxidation is shown in red. The open circles represent the raw data (only every 10th point is shown for clarity), and the solid traces are corrected for the effects of HO_2 self-reaction. The solid traces therefore represent a minimum HO_2 production needed to generate the observed signal. At the higher O_2 concentration shown on the right, more HO_2 is produced than the initial Cl atom concentration, a signature of chain branching.

at first glance, but the reactivity of the OH product provides a strong kinetic bias for detection of the more rapid direct formation pathways. Figure 15 shows the modeled OH formation from neopentane oxidation at 671 K with and without the formally direct pathways, for the ad hoc model and for the model using the kinetic results of Sun and Bozzelli.[80] In both models, the chemically activated path from the neopentyl and O_2 reactants directly to OH + 3,3-dimethyloxetane is required to accurately model the OH formation. The ad hoc model predicts a much larger direct component than the steady-state QRRK-based model of Sun and Bozzelli.[80] As the ad hoc model is based on multiple-well time-dependent master equation models on the related *n*-propyl + O_2 system,[37−39,56] it would be informative to learn whether such rigorous kinetics computations on the neopentyl + O_2 system yield similarly large direct components.

The formally direct pathways to bimolecular products imply that other direct pathways also occur, for example, from R + O_2 directly to QOOH. The consequences of these direct pathways have not been thoroughly explored, but they may have substantial impact on secondary reactions of the hydroperoxyalkyl species with oxygen. Discerning these effects in photolytically initiated oxidation experiments will require extension of the modeling to include these subsequent reactions and may require new methods that monitor more intermediate species.

Reactions of QOOH. The reactions of the somewhat ephemeral QOOH species are critical for chain branching at low temperature. A possible means for investigating these reactions experimentally is suggested by studies of HO_2 formation in Cl-initiated neopentane oxidation.[56] As neopentyl + O_2 cannot directly form HO_2, any HO_2 observed must arise from secondary reactions, including those of the QOOH species. Figure 16 shows measurements of HO_2 formation in Cl-initiated neopentane oxidation at two different oxygen concentrations. The HO_2 signals have been partially corrected for ongoing removal by the HO_2 self-reaction, yielding the minimum production of HO_2 necessary to produce the observed signal. The reference reaction of Cl-initiated methanol oxidation produces an amount of HO_2 equal to the initial Cl atom concentration. At the higher oxygen concentration, the HO_2 production continues throughout the full experimental time scale, eventually producing more HO_2 radicals than Cl atoms produced in the photolysis. This is clear evidence of chain branching. The increase in HO_2 production as the O_2 concentration is increased is consistent with branching via a second O_2 addition to the QOOH radical. The ad hoc model used to model the OH formation in the neopentane oxidation has also been applied to the HO_2 formation. Most of the HO_2 in the model is formed by the reaction of OH radicals with the neopentylperoxy radical

$$OH + C_5H_{11}OO \rightarrow HO_2 + C_5H_{11}O \qquad (8)$$

followed by rapid dissociation of the neopentoxy radical ($C_5H_{11}O$). Reaction 8 and its analogues for other alkylperoxy radicals have not been widely included in models of hydrocarbon oxidation; including these reactions might change the interpretation of some previous kinetic measurements. In the present case, the radical density is high enough that reaction 8 makes a substantial contribution to the RO_2 removal. The ad hoc model successfully predicts the HO_2 formation at low O_2 concentrations but fails to model the increase in HO_2 at higher O_2 concentrations, suggesting that the model inaccurately treats the QOOH chemistry. It is possible that more detailed calculations of the QOOH reaction rate coefficients will improve the agreement, and with improved modeling, experiments may be designed to focus more closely on the QOOH reactions. Some current efforts in that direction are described in the next section.

Future Directions

New Experimental Techniques. The interpretation of the HO_2 production in the neopentane system highlights the necessity of following secondary chemical pathways in complicated systems such as photolytically initiated oxidation. Indeed, the secondary chemistry of the QOOH species is one of the key unsolved questions in modeling ignition chemistry and low-temperature oxidation. As the oxidation proceeds, the number of transiently generated species increases; monitoring HO_2 and OH is insufficient characterization of such a complex reaction mixture.

A new apparatus has recently been constructed that promises to enable isomer-resolved detection of the time-resolved concentrations of multiple intermediates and primary and secondary products of photolytically initiated reactions. Designed by David Osborn from the Combustion Research Facility of Sandia National Laboratories, in collaboration with the author and with scientists at the Advanced Light Source at Lawrence Berkeley National Laboratory, this instrument uses the powerful method of synchrotron photoionization mass spectrometry to analyze the reacting mixture. Photoionization mass spectrometry with synchrotron radiation has proved extraordinarily valuable in molecular beam mass sampling investigations of flame chemistry, providing unprecedented detail about the isomeric nature of combustion intermediates.[87−91] The new kinetics apparatus applies laser photolysis/photoionization mass spectrometry methods employed by several other groups[20,92−94] but uses a novel magnetic sector mass spectrometer[95,96] to collect multiple masses simultaneously. This multiple-mass capability can reveal side reactions or unexpected products that might be overlooked in experiments that use single-mass detection.

The reaction is initiated by laser photolysis in a low-pressure tube. The contents of the reactor are continuously sampled in an effusive beam emitted through a small hole in the side of the tube. The emitted molecules are ionized by the tunable vacuum ultraviolet light from the Chemical Dynamics Beamline of the Advanced Light Source. The undulator radiation from

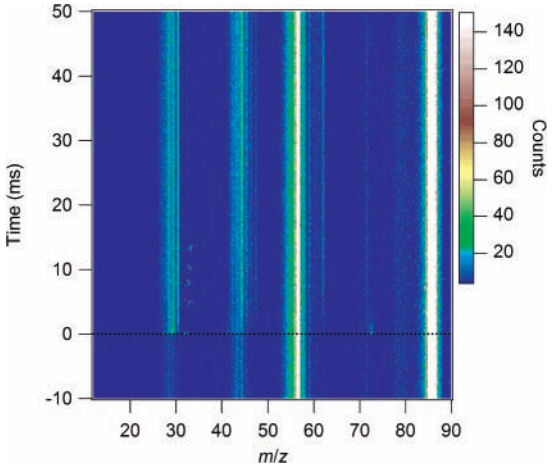

Figure 17. Time-resolved photoionization mass spectrum from 193 nm photolysis of 3-pentanone in the presence of O_2, taken at a photon energy of 11 eV. The simultaneous detection of multiple masses allows competing side and secondary reactions to be analyzed.

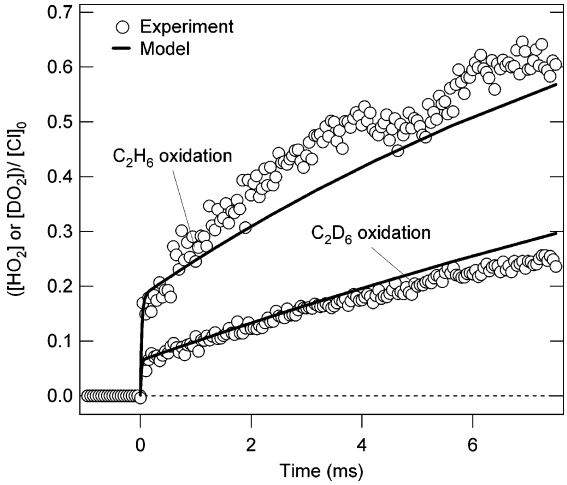

Figure 18. Comparison of DO_2 formation[77] from Cl-initiated oxidation of C_2D_6 with HO_2 formation from C_2H_6 oxidation.[27] The open circles represent the experimental data, normalized to the initial Cl atom concentration and approximately corrected for self-reaction and removal by reaction with RO_2, as described in the text. The solid lines are results from solutions to the time-resolved master equation.

the synchrotron passes through a rare gas filter to remove higher harmonics[97,98] and is dispersed by a 3 m monochromator. The photoions are separated by mass in a double-focusing spectrometer of the Mattauch−Herzog geometry[95,96] and are collected on a time- and position-sensitive detector. A preliminary result from this machine is displayed in Figure 17, depicting primary and secondary product formation in a photolytically initiated ethyl oxidation system. Photolysis of 3-pentanone (diethyl ketone) at 193 nm forms two ethyl radicals and initiates the reaction. The oxygen concentration is high enough that the rise of products from the reaction of ethyl with O_2 is unresolved. The subsequent reactions of the ethylperoxy radicals can be clearly followed by the rise in acetaldehyde and other secondary or tertiary products; furthermore, the side reactions of C_2H_5CO radicals are also evident. The photoionization efficiency curves can be used to identify individual isomers for a particular mass.[87,90,91] The nearly universal and isomer-specific detection provided by tunable photoionization mass spectrometry, combined with the simultaneous detection of multiple masses, promises to make this multiplexed chemical kinetics reactor a powerful tool for investigating complicated chemical reaction systems such as alkyl radical reactions with O_2.

Kinetic Isotope Effects. The kinetic isotope effects for product formation can provide additional data with which to refine the theoretical estimates of R + O_2 chemistry. The formation of DO_2 has recently been measured in the Cl-initiated oxidation of deuterated ethane and propane, as well as from the photolysis of deuterated 1-iodopropane and 2-iodopropane.[77] Under the Born−Oppenheimer approximation, the potential energy surface for the deuterated reactants must be the same as that for the hydrogenated reactants, but the energy transfer kinetics may be very different. Figure 18 shows the formation of DO_2 from Cl-initiated oxidation of C_2D_6[77] compared to the HO_2 formation from its hydrogenated counterpart.[27] These traces are approximately corrected for self-reaction and reactions of the HO_2 or DO_2 with the alkylperoxy radical, as described above. The figure focuses on the early time after the photolysis, when effects of the relatively poorly characterized reactions of the deuterated RO_2 radicals are small, and the extracted production depends predominantly on the R + O_2 reaction. The smaller prompt yield and slower secondary production of DO_2 relative to that of HO_2 is principally a consequence of the larger density of states in the deuterated ethylperoxy radical. Master equation solutions using the same stationary point energies satisfactorily model the product formation from both isotopomers.[77] Future work may use partially deuterated reagents to isolate contributions to OH or HO_2 production from individual sites in the alkyl radical.

Automated Generation of Larger Reaction Mechanisms. The consideration of the QOOH chemistry that is essential to describing ignition phenomena leads inevitably to the need to model secondary chemistry in alkyl oxidation, and to design experiments that probe these key chemical steps. In this area, we have begun collaboration with the group of Prof. William Green at the Massachusetts Institute of Technology to apply automated reaction mechanism generation (RMG) methods[69,70,73] to the study of HO_2 and OH formation in neopentane oxidation. The automatic generation of reaction mechanisms uses approximate kinetic methods such as rule-based estimates[99−101] or other a priori methods[72,102−105] to estimate rate coefficients and analyzes which reactions are to be retained in the final mechanism based on some criterion of their importance.[73,106,107] After generation of a sufficient system of kinetic equations, analysis of the sensitivity of experimental observables to individual rate coefficients can guide the design of new experiments. Higher-level computational work can also be performed to provide rigorous rate coefficient estimates for the most critical reactions in the system. Preliminary results[108] modeling Cl-initiated oxidation of neopentane with an automatically generated reaction mechanism of approximately 65 species and 600 reactions show heartening agreement with the chain branching signature of increased HO_2 production at higher O_2 densities and suggest that the HO_2 and OH profiles are both sensitive to the addition of O_2 to the QOOH species. New measurements of product formation in neopentane oxidation, currently underway, may improve the experimental focus on the important QOOH reactions.

Direct QOOH Detection. Perhaps foremost among the goals that have eluded researchers of alkyl + O_2 reactions is the direct detection of hydroperoxyalkyl radicals. The spectroscopy of the QOOH radicals remains unknown; calculations of electronic and vibrational spectra of representative QOOH molecules would be helpful to guide experimental investigations. The central technical challenge in detection of QOOH species is their instability and hence their low steady-state concentrations in standard oxidation systems. It seems likely that the first

successful detection of QOOH will come from a well-designed low-temperature experiment, for example, in a supersonic expansion or in He droplets. Production of QOOH in such an environment will pose challenges of its own; formation from HO_2 + alkene must traverse a large energy barrier, and formation from R + O_2 will suffer from small yields. Nevertheless, an experimental spectrum of any QOOH molecule has the potential to be ground-breaking.

Investigation of QOOH molecules in a reacting mixture by optical means would almost certainly require a strong electronic transition. Alternatively, photoionization mass spectrometry may be able to resolve the QOOH isomer from the RO_2 isomer. Again, the ionization energies of the QOOH species are unknown, and calculations are needed to assess whether photoionization detection could be feasible. Ab initio calculation of ionization energies can be very accurate,[109] and such calculations have been instrumental in the identification of isomers in flames.[90,110,111] Calculated ionization energies, combined with an experimental verification of QOOH photoionization, possibly in a molecular beam experiment, could open the door for mass spectrometric measurements of this elusive intermediate.

Conclusions

The mechanisms of the reactions of alkyl radicals with molecular oxygen have been the subject of study and speculation for decades. The combination of new experimental measurements of product formation in pulsed-photolytically initiated oxidation reaction and state-of-the-art computational kinetics using ab initio calculations of stationary point characteristics has uncovered new aspects of key steps in these mechanisms. However, some fascinating questions remain, especially concerning the rate constants for formation and reactions of the elusive but critically important hydroperoxyalkyl radical intermediates. New experimental and theoretical tools are emerging that may answer these questions and very likely also uncover new puzzles in the complicated chemistry of hydrocarbon oxidation.

Acknowledgment. The co-workers and collaborators who have performed the experiments on these reactions are gratefully acknowledged: Sandia postdoctoral associates Dr. Eileen P. Clifford, Dr. John T. Farrell, Dr. John D. DeSain, and Dr. Edgar G. Estupiñán; Prof. Atsumu Tezaki (University of Tokyo), who visited the Combustion Research Facility in 2001; student interns Jared D. Smith (presently at University of California, Berkeley) and Huzeifa Ismail (Massachusetts Institute of Technology); and laboratory support physicist Leonard E. Jusinski. The theoretical and computational work of Dr. Stephen J. Klippenstein (Argonne National Laboratory) and Dr. James A. Miller (Sandia National Laboratories) has been indispensable in turning the laboratory measurements into meaningful scientific data. I thank Dr. David L. Osborn (Sandia National Laboratories) for agreeing to the use of preliminary images of our new work from the Advanced Light Source. I also thank Prof. William H. Green, Huzeifa Ismail, and Sarah V. Petway (Massachusetts Institute of Technology) for sharing their results on reaction mechanism generation for the neopentane oxidation system. This work is supported by the Division of Chemical Sciences, Geosciences, and Biosciences, the Office of Basic Energy Sciences, the U. S. Department of Energy. Sandia is a multi-program laboratory operated by Sandia Corporation, a Lockheed Martin Company, for the National Nuclear Security Administration under contract DE-AC04-94-AL85000.

Supporting Information Available: Mathematical description of the approximate inversion of HO_2 signals to extract time-resolved HO_2 production. This material is available free of charge via the Internet at http://pubs.acs.org.

Note Added after ASAP Publication. This manuscript was originally published on the Web March 1, 2006. The manuscript was reposted March 9, 2006 with revised terms in eq 7.

References and Notes

(1) Atkinson, R. *Atmos. Environ.* **2000**, *34*, 2063.
(2) Miller, J. A.; Pilling, M. J.; Troe, J. *Proc. Combust. Inst.* **2005**, *30*, 43.
(3) Walker, R. W.; Morley, C. Basic Chemistry of Combustion. In *Low-Temperature Combustion and Autoignition*; Pilling, M. J., Ed.; Elsevier: Amsterdam, The Netherlands, 1997; pp 1−124.
(4) Walker, R. W. Some Burning Problems in Combustion Chemistry. In *Research in Chemical Kinetics*; Compton, R., Hancock, G., Eds.; Elsevier: Amsterdam, The Netherlands, 1995; Vol. 3, pp 1−68.
(5) Miller, J. A.; Klippenstein, S. J.; Robertson, S. H. *Proc. Combust. Inst.* **2000**, *28*, 1479.
(6) Miller, J. A.; Klippenstein, S. J. *Int. J. Chem. Kinet.* **2001**, *33*, 654.
(7) Westbrook, C. K. *Proc. Combust. Inst.* **2000**, *28*, 1563.
(8) Pitz, W. J.; Westbrook, C. K. *Combust. Flame* **1986**, *63*, 113.
(9) Pollard, R. T. Hydrocarbons. In *Gas-Phase Combustion*; Bamford, C. H., Tipper, C. F. H., Eds.; Elsevier: Amsterdam, The Netherlands, 1977; pp 249−440.
(10) Benson, S. W. *Adv. Chem. Ser.* **1968**, *76*, 143.
(11) Plumb, I. C.; Ryan, K. R. *Int. J. Chem. Kinet.* **1981**, *13*, 1011.
(12) Kaiser, E. W.; Lorkovic, I. M.; Wallington, T. J. *J. Phys. Chem.* **1990**, *94*, 3352.
(13) Kaiser, E. W.; Wallington, T. J.; Andino, J. M. *Chem. Phys. Lett.* **1990**, *168*, 309.
(14) Kaiser, E. W. *J. Phys. Chem.* **1995**, *99*, 707.
(15) Baldwin, R. R.; Pickering, I. A.; Walker, R. W. *J. Chem. Soc., Faraday Trans. 1* **1980**, *76*, 2374.
(16) Gulati, S. K.; Walker, R. W. *J. Chem. Soc., Faraday Trans. 2* **1988**, *84*, 401.
(17) Handford-Styring, S. M.; Walker, R. W. *Phys. Chem. Chem. Phys.* **2001**, *3*, 2043.
(18) McAdam, K. G.; Walker, R. W. *J. Chem. Soc., Faraday Trans. 2* **1987**, *83*, 1509.
(19) Wagner, A. F.; Slagle, I. R.; Sarzynski, D.; Gutman, D. *J. Phys. Chem.* **1990**, *94*, 1853.
(20) Slagle, I. R.; Feng, Q.; Gutman, D. *J. Phys. Chem.* **1984**, *88*, 3648.
(21) Baldwin, R. R.; Walker, R. W. *Proc. Combust. Inst.* **1978**, *17*, 525.
(22) Baldwin, R. R.; Hisham, M. W. M.; Walker, R. W. *Proc. Combust. Inst.* **1984**, *20*, 743.
(23) Baldwin, R. R.; Stout, D. R.; Walker, R. W. *J. Chem. Soc., Faraday Trans.* **1991**, *87*, 2147.
(24) Walker, R. W. *Proc. Combust. Inst.* **1988**, *22*, 883.
(25) Baldwin, R. R.; Dean, C. E.; Walker, R. W. *J. Chem. Soc., Faraday Trans. 2* **1986**, *82*, 1445.
(26) DeSain, J. D.; Clifford, E. P.; Taatjes, C. A. *J. Phys. Chem. A* **2001**, *105*, 3205.
(27) Clifford, E. P.; Farrell, J. T.; DeSain, J. D.; Taatjes, C. A. *J. Phys. Chem. A* **2000**, *104*, 11549.
(28) DeSain, J. D.; Taatjes, C. A. *J. Phys. Chem. A* **2001**, *105*, 6646.
(29) Estupiñán, E. G.; Klippenstein, S. J.; Taatjes, C. A. *J. Phys. Chem. B* **2005**, *109*, 8374.
(30) Kaiser, E. W. *J. Phys. Chem. A* **2002**, *106*, 1256.
(31) Ignatyev, I. S.; Xie, Y.; Allen, W. D.; Schaefer, H. F., III. *J. Chem. Phys.* **1997**, *107*, 141.
(32) Rienstra-Kiracofe, J. C.; Allen, W. D.; Schaefer, H. F., III. *J. Phys. Chem. A* **2000**, *104*, 9823.
(33) Cullis, C. F.; Saeed, M.; Trimm, D. L. *Proc. R. Soc. London, Ser. A* **1967**, *300*, 455.
(34) Cullis, C. F.; Fish, A.; Saeed, M.; Trimm, D. L. *Proc. R. Soc. London, Ser. A* **1966**, *289*, 402.
(35) Hughes, K. J.; Halford-Maw, P. A.; Lightfoot, P. D.; Turanyi, T.; Pilling, M. J. *Proc. Combust. Inst.* **1992**, *24*, 645.
(36) Berry, T.; Cullis, C. F.; Trimm, D. L. *Proc. R. Soc. London, Ser. A* **1970**, *316*, 377.
(37) DeSain, J. D.; Taatjes, C. A.; Miller, J. A.; Klippenstein, S. J.; Hahn, D. K. *Faraday Discuss.* **2001**, *119*, 101.
(38) DeSain, J. D.; Klippenstein, S. J.; Miller, J. A.; Taatjes, C. A. *J. Phys. Chem. A* **2003**, *107*, 4415.
(39) DeSain, J. D.; Klippenstein, S. J.; Miller, J. A.; Taatjes, C. A. *J. Phys. Chem. A* **2004**, *108*, 7127.

(40) Berkowitz, J.; Ellison, G. B.; Gutman, D. *J. Phys. Chem.* **1994**, *98*, 2744.
(41) Tyndall, G. S.; Orlando, J. J.; Wallington, T. J.; Dill, M.; Kaiser, E. W. *Int. J. Chem. Kinet.* **1997**, *29*, 43.
(42) Hughes, K. J.; Lightfoot, P. D.; Pilling, M. J. *Chem. Phys. Lett.* **1992**, *191*, 581.
(43) Seakins, P. W.; Robertson, S. H.; Pilling, M. J.; Slagle, I. R.; Gmurczyk, G. W.; Bencsura, A.; Gutman, D.; Tsang, W. *J. Phys. Chem.* **1993**, *97*, 4450.
(44) Slagle, I. R.; Park, J.-Y.; Gutman, D. *Proc. Combust. Inst.* **1984**, *20*, 733.
(45) Slagle, I. R.; Ratajczak, E.; Gutman, D. *J. Phys. Chem.* **1986**, *90*, 402.
(46) Cooper, D. E.; Watjen, J. P. *Opt. Lett.* **1986**, *11*, 606.
(47) Janik, G. R.; Carlisle, C. B.; Gallagher, T. F. *J. Opt. Soc. Am. B* **1986**, *3*, 1070.
(48) Powers, P. E.; Taatjes, C. A.; Kulp, T. J. *Appl. Opt.* **1996**, *35*, 4735.
(49) DeSain, J. D.; Ho, A. D.; Taatjes, C. A. *J. Mol. Spectrosc.* **2003**, *219*, 163.
(50) Fink, E. H.; Ramsay, D. A. *J. Mol. Spectrosc.* **1997**, *185*, 304.
(51) Bjorklund, G. C. *Opt. Lett.* **1980**, *5*, 15.
(52) Hall, G. E.; North, S. *Annu. Rev. Phys. Chem.* **2000**, *51*, 243.
(53) Taatjes, C. A.; Oh, D. B. *Appl. Opt.* **1997**, *36*, 5817.
(54) Pilgrim, J. S.; Jennings, R. T.; Taatjes, C. A. *Rev. Sci. Instrum.* **1997**, *68*, 1875.
(55) Herriott, D.; Kogelnik, H.; Kompfner, R. *Appl. Opt.* **1964**, *3*, 523.
(56) DeSain, J. D.; Klippenstein, S. J.; Taatjes, C. A. *Phys. Chem. Chem. Phys.* **2003**, *5*, 1584.
(57) DeSain, J. D.; Klippenstein, S. J.; Taatjes, C. A.; Hurley, M. D.; Wallington, T. J. *J. Phys. Chem. A* **2003**, *107*, 1992.
(58) Ha, T.-K.; He, Y.; Pochert, J.; Quack, M.; Ranz, R.; Seyfang, G.; Thanopoulos, I. *Ber. Bunsen-Ges. Phys. Chem.* **1995**, *99*, 384.
(59) Carstensen, H.-H.; Naik, C. V.; Dean, A. M. *J. Phys. Chem. A* **2005**, *109*, 2264.
(60) Klippenstein, S. J.; Miller, J. A. *J. Phys. Chem. A* **2002**, *106*, 9267.
(61) Klippenstein, S. J.; Wagner, A. F.; Dunbar, R. C.; Wardlaw, D. M.; Robertson, S. H.; Miller, J. A. *VARIFLEX*, 1.12m ed.; 2002.
(62) Klippenstein, S. J.; Miller, J. A. *J. Phys. Chem. A* **2005**, *109*, 4285.
(63) Miller, J. A.; Klippenstein, S. J.; Raffy, C. *J. Phys. Chem. A* **2002**, *106*, 4904.
(64) Miller, J. A.; Klippenstein, S. J. *J. Phys. Chem. A* **2003**, *107*, 2680.
(65) Klippenstein, S. J. *J. Chem. Phys.* **1992**, *96*, 367.
(66) Klippenstein, S. J.; Allen, W. D. *Ber. Bunsen-Ges. Phys. Chem.* **1997**, *101*, 423.
(67) Klippenstein, S. J. *Chem. Phys. Lett.* **1993**, *214*, 418.
(68) Taatjes, C. A.; Klippenstein, S. J. *J. Phys. Chem. A* **2001**, *105*, 8567.
(69) Green, W. H.; Barton, P. I.; Bhattacharjee, B.; Matheu, D. M.; Schwer, D. A.; Song, J.; Sumathi, R.; Carstensen, H.-H.; Dean, A. M.; Grenda, J. M. *Ind. Eng. Chem. Res.* **2001**, *40*, 5362.
(70) Susnow, R. G.; Dean, A. M.; Green, W. H.; Peczak, P.; Broadbelt, L. J. *J. Phys. Chem. A* **1997**, *101*, 3731.
(71) Venkatesh, P. K.; Dean, A. M.; Cohen, M. H.; Carr, R. W. *J. Chem. Phys.* **1999**, *111*, 8313.
(72) Bozzelli, J. W.; Dean, A. M. *J. Phys. Chem.* **1990**, *94*, 3313.
(73) Tomlin, A. S.; Turányi, T.; Pilling, M. J. Mathematical Tools for the Construction, Investigation, and Reduction of Combustion Mechanisms. In *Low-Temperature Combustion and Autoignition*; Pilling, M. J., Ed.; Elsevier: Amsterdam, The Netherlands, 1997; Vol. 35.
(74) Kaiser, E. W.; Wallington, T. J. *J. Phys. Chem.* **1996**, *100*, 18770.
(75) Kaiser, E. W. *J. Phys. Chem. A* **1998**, *102*, 5903.
(76) Knyazev, V. D.; Slagle, I. R. *J. Phys. Chem. A* **1998**, *102*, 1770.
(77) Estupiñán, E. G.; Smith, J. D.; Tezaki, A.; Jusinski, L. E.; Klippenstein, S. J.; Taatjes, C. A. Measurements and Modeling of DO_2 Formation in the Reactions of C_2D_5 and C_3D_7 Radicals with O_2. Manuscript in preparation.
(78) Baker, R. R.; Baldwin, R. R.; Walker, R. W. *Trans. Faraday Soc.* **1970**, *66*, 3016.
(79) Bozzelli, J. W.; Sheng, C. *J. Phys. Chem. A* **2002**, *106*, 1113.
(80) Sun, H.; Bozzelli, J. W. *J. Phys. Chem. A* **2004**, *108*, 1694.
(81) Baker, R. R.; Baldwin, R. R.; Walker, R. W. *J. Chem. Soc., Faraday Trans. 1* **1975**, *71*, 756.
(82) Baker, R. R.; Baldwin, R. R.; Fuller, A. R.; Walker, R. W. *J. Chem. Soc., Faraday Trans. 1* **1975**, *71*, 736.
(83) Baker, R. R.; Baldwin, R. R.; Everett, C. J.; Walker, R. W. *Combust. Flame* **1975**, *25*, 285.
(84) Baker, R. R.; Baldwin, R. R.; Walker, R. W. *Combust. Flame* **1976**, *27*, 147.
(85) Baldwin, R. R.; Hisham, M. W. M.; Walker, R. W. *J. Chem. Soc., Faraday Trans. 1* **1982**, *78*, 1615.
(86) See comments by Taatjes, C. A. and Griffiths, J. F. in *Faraday Discuss.* **2001**, *119*, 356.
(87) Cool, T. A.; Nakajima, K.; Mostefaoui, T. A.; Qi, F.; McIlroy, A.; Westmoreland, P. R.; Law, M. E.; Poisson, L.; Peterka, D. S.; Ahmed, M. *J. Chem. Phys.* **2003**, *119*, 8356.
(88) Cool, T. A.; Nakajima, K.; Taatjes, C. A.; McIlroy, A.; Westmoreland, P. R.; Law, M. E.; Morel, A. *Proc. Combust. Inst.* **2005**, *30*, 1681.
(89) Cool, T. A.; McIlroy, A.; Qi, F.; Westmoreland, P. R.; Poisson, L.; Peterka, D. S.; Ahmed, M. *Rev. Sci. Instrum.* **2005**, *76*, 094102.
(90) Taatjes, C. A.; Klippenstein, S. J.; Hansen, N.; Miller, J. A.; Cool, T. A.; Wang, J.; Law, M. E.; Westmoreland, P. R. *Phys. Chem. Chem. Phys.* **2005**, *7*, 806.
(91) Taatjes, C. A.; Hansen, N.; McIlroy, A.; Miller, J. A.; Senosiain, J. P.; Klippenstein, S. J.; Qi, F.; Sheng, L.; Zhang, Y.; Cool, T. A.; Wang, J.; Westmoreland, P. R.; Law, M. E.; Kasper, T.; Kohse-Höinghaus, K. *Science* **2005**, *308*, 1887.
(92) Slagle, I. R.; Yamada, F.; Gutman, D. *J. Am. Chem. Soc.* **1981**, *103*, 149.
(93) Ruiz, R. P.; Bayes, K. D. *J. Phys. Chem.* **1984**, *88*, 2592.
(94) Washida, N.; Martinez, R. I.; Bayes, K. B. *Z. Naturforsch., A* **1974**, *29*, 251.
(95) Sinha, M. P.; Tomassian, A. D. *Rev. Sci. Instrum.* **1991**, *62*, 2618.
(96) Sinha, M. P.; Houseman, J. *Proc. SPIE* **2003**, *5048*, 119.
(97) Suits, A. G.; Heimann, P.; Yang, X.; Evans, M.; Hsu, C.-W.; Lu, K.-t.; Lee, Y. T.; Kung, A. H. *Rev. Sci. Instrum.* **1995**, *66*, 4841.
(98) Heimann, P. A.; Koike, M.; Hsu, C. W.; Blank, D.; Yang, X. M.; Suits, A. G.; Lee, Y. T.; Evans, M.; Ng, C. Y.; Flaim, C.; Padmore, H. A. *Rev. Sci. Instrum.* **1997**, *68*, 1945.
(99) Sumathi, R.; Carstensen, H.-H.; Green Jr., W. H. *J. Phys. Chem. A* **2001**, *105*, 8969.
(100) Sumathi, R.; Carstensen, H.-H.; Green Jr., W. H. *J. Phys. Chem. A* **2002**, *106*, 5474.
(101) Sumathi, R.; Carstensen, H.-H.; Green, W. H., Jr. *J. Phys. Chem. A* **2001**, *105*, 6910.
(102) Sumathi, R.; Green, W. H., Jr. *Theor. Chem. Acc.* **2002**, *108*, 187.
(103) Wijaya, C. D.; Sumathi, R.; Green, W. H., Jr. *J. Phys. Chem. A* **2003**, *107*, 4908.
(104) Matheu, D. M.; Green, W. H., Jr.; Grenda, J. M. *Int. J. Chem. Kinet.* **2003**, *35*, 95.
(105) Dean, A. M.; Westmoreland, P. R. *Int. J. Chem. Kinet.* **1987**, *19*, 207.
(106) Bhattacharjee, B.; Schwer, D. A.; Barton, P. I.; Green, W. H., Jr. *Combust. Flame* **2001**, *135*, 191.
(107) Schwer, D. A.; Lu, P.; Green, W. H., Jr. *Combust. Flame* **2003**, *133*, 451.
(108) Green, W. H.; Ismail, H.; Petway, S. V. Personal communication.
(109) Lau, K.-C.; Ng, C. Y. *J. Chem. Phys.* **2005**, *122*, 224310.
(110) Taatjes, C. A.; Osborn, D. L.; Cool, T. A.; Nakajima, K. *Chem. Phys. Lett.* **2004**, *394*, 19.
(111) Hansen, N.; Klippenstein, S. J.; Taatjes, C. A.; Miller, J. A.; Wang, J.; Cool, T. A.; Yang, B.; Yang, R.; Wei, L.; Huang, C.; Wang, J.; Qi, F.; Law, M. E.; Westmoreland, P. R. *J. Phys. Chem. A* **2006**, *110*, 3670.